Journal of Computer Science and Electrical Engineering
Print ISSN: 2663-1938
Online ISSN: 2663-1946
DOI: https://doi.org/10.61784/jcsee3124

MOTION COMPENSATION FOR OPTICAL COHERENCE TOMOGRAPHY ANGIOGRAPHY BASED ON MULTI-DIMENSIONAL MATRIX PENCIL METHOD AND ADAPTIVE EN-FACE IMAGE ENHANCEMENT

LinKang Du, Lei Liu, HaiYi Bian*
School of Electronic and Information Engineering, Huaiyin Institute of Technology, Huai'an 223001, Jiangsu, China.
**Corresponding Author: HaiYi Bian*

Abstract: This paper proposes a two-stage algorithm combining the multi-dimensional matrix pencil method (MDMP) with En-face image enhancement to address the problem of eye motion artifacts severely degrading image quality in optical coherence tomography angiography (OCTA). In the first stage, a two-dimensional Hankel matrix pencil in the depth-time domain is constructed to jointly estimate Doppler frequency shifts and motion parameters of blood flow signals. The Centro-Hermitian property is exploited via unitary transformation to reduce computational complexity by approximately 75%, and an automatic parameter pairing mechanism is introduced to avoid mispairing problems inherent in conventional approaches. In the second stage, En-face image enhancement is applied to the MDMP-compensated retinal volume data, sequentially performing FFT difference calculation, weighted layered projection, CLAHE adaptive enhancement, column-wise median normalization for stripe removal, and FAZ region cosine gradient darkening to generate high-quality En-face vascular images. Experimental validation on a retinal OCTA dataset demonstrates that compared with multiple existing methods, the proposed method achieves a 65.1% improvement in signal-to-noise ratio (SNR), an 80.2% improvement in contrast-to-noise ratio (CNR), a structural similarity index (SSIM) of 0.94, and a 34.0% reduction in motion artifact index (MAI). The results confirm that the proposed two-stage algorithm effectively suppresses eye motion artifacts and significantly enhances OCTA En-face vascular imaging quality.
Keywords: Optical coherence tomography angiography; Multi-dimensional matrix pencil method; En-face image enhancement; Weighted layered projection; CLAHE; FAZ processing; Motion compensation; Retinal imaging

1 INTRODUCTION

Optical coherence tomography angiography (OCTA) is a non-invasive vascular imaging technique that achieves three-dimensional visualization of retinal and choroidal microvasculature without contrast agents, using moving red blood cells as an endogenous contrast agent to detect inter-B-scan signal differences [1-3]. Existing OCTA algorithms span three categories: phase-based methods (e.g., Doppler OCT, phase variance), which are sensitive to bulk-motion noise; amplitude-based methods such as SSADA, which tolerate bulk motion but sacrifice axial resolution; and complex-signal-based methods such as OMAG and CDV, which exploit both amplitude and phase for higher sensitivity [4-5]. Despite these advances, OCTA image quality is severely degraded by eye motion artifacts (microsaccades, drift, tremor), speckle noise, and projection artifacts, all of which limit clinical utility [6-7].

Motion compensation strategies include hardware tracking, image registration, and signal processing methods, each with limitations in cost, robustness, or resolution [8-12]. The matrix pencil method (MP), originally developed for parameter estimation of complex exponentials, has been extended to multi-dimensional scenarios (MDMP) for massive MIMO channel prediction and further equipped with automatic parameter pairing [13, 14], providing a strong theoretical basis for joint multi-parameter estimation. However, its application to OCTA motion compensation remains unexplored.

Motivated by the above developments, this paper proposes a two-stage algorithm combining MDMP with En-face image enhancement. The first stage employs MDMP to jointly estimate blood flow signal parameters and motion parameters for compensation of major motion artifacts. The second stage generates high-quality En-face images through FFT difference calculation, weighted layered projection, CLAHE enhancement, stripe removal, and FAZ gradient processing. The main contributions of this work are: (1) the first application of the multi-dimensional matrix pencil method to OCTA motion compensation for joint estimation of blood flow and motion parameters; (2) an SNR-guided phase compensation strategy that uses the phase difference of high-SNR tissue regions for bulk-motion correction; (3) an En-face image enhancement pipeline centered on weighted layered projection and integrating CLAHE enhancement with FAZ gradient processing, preserving capillary details while suppressing background noise and FAZ artifacts.

2 THEORETICAL BACKGROUND

2.1 OCTA Signal Model

OCTA detects blood flow by analyzing signal changes between consecutive B-scans. Let the complex OCT signal at depth position z and time t be s(z, t). In the presence of blood flow and tissue motion, the signal is modeled as:

$$s(z,t) = \Sigma_p \alpha_p \, exp(j2\pi\omega_p t) \, exp(-j2\pi f_p z) + n(z,t) \quad (1)$$

where P is the number of signal components; α_p is the complex amplitude of the p-th component; ω_p is the Doppler frequency shift related to blood flow velocity; f_p is the depth frequency; and n(z,t) is additive noise. When eye motion is present, the Doppler frequency shift ω_p becomes a time-varying parameter $\omega_p(t) = \omega_{p,0} + \Delta\omega_p(t)$, where $\Delta\omega_p(t)$ is the motion-induced frequency shift variation.

2.2 Multi-dimensional Matrix Pencil Method

The multi-dimensional matrix pencil method constructs multi-dimensional Hankel matrices to jointly estimate multiple parameters. For a two-dimensional signal v(a, b), a Hankel matrix is first constructed along the first dimension, then stacked along the second dimension to form an enhanced matrix:

$$D_e = [D_0^T, D_1^T, \ldots, D(K-1)^T]^T = F_1 \, A \, F_2 \quad (2)$$

where K is the pencil parameter along the second dimension; F_1 and F_2 are combined structural matrices; and A is a diagonal amplitude matrix. The pencil parameters must satisfy: $P < L < N_1 - P + 1$ and $P < K < N_2 - P + 1$, where N_1 and N_2 are the sample counts in the two dimensions and P is the expected number of signal components.

2.3 Unitary Transformation Optimization

To reduce computational complexity, a unitary transformation is applied exploiting the Centro-Hermitian property of the signal. A Centro-Hermitian extended matrix $D\_ch = [D_e : \Pi_m D_e * \Pi_n]$ is first constructed, then the unitary transformation yields a real-valued matrix:

$$D_r = Q_m H \, D\_ch \, Q_{2n} \quad (3)$$

where D_r is a real-valued matrix whose SVD decomposition and eigenvalue computation can be performed entirely in the real domain. The unitary transformation converts complex arithmetic to real arithmetic, reducing computational complexity from $O(8n^3)$ to $O(2n^3)$, a reduction of approximately 75%.

2.4 Automatic Parameter Pairing

The key challenge in multi-dimensional parameter estimation is correctly pairing parameters across different dimensions. This paper employs eigenvector structural similarity for automatic pairing. After SVD decomposition of the real matrix D_r, parameters are estimated by solving the generalized eigenvalue problem of real matrix pencils. A shared eigenvector matrix ensures correct correspondence of parameters across dimensions:

$$\Phi_\gamma = W_u^{-1} (K_3 J \, U_{rs}) \dagger (K_4 J \, U_{rs}) \, W_u \quad (4)$$

2.5 En-face Image Enhancement Pipeline

After MDMP motion compensation, En-face image enhancement is applied to the compensated volume data through five sequential steps: FFT difference calculation, weighted layered projection, stripe removal, CLAHE adaptive enhancement, and FAZ gradient processing.

(1) FFT difference calculation: A one-dimensional FFT is applied along the depth direction for each set of six consecutive B-scans, and the amplitude is computed. The effective frequency range (rows 101–450) is extracted; the mean amplitude difference of three adjacent frame pairs is computed and then denoised by Gaussian filtering ($\sigma = 0.01$), yielding a decorrelation image D(z, x) that separates blood flow signals from the static tissue background in the frequency domain.

(2) Weighted layered projection: Pre-fitted retinal layer boundary curves determine the upper and lower boundaries for each A-scan. Within the boundary interval, maximum intensity projection (MIP) and average intensity projection (AVP) are computed and combined with weights:

$$P(x,t) = w_0 \cdot MIP(x,t) + w_1 \cdot AVP(x,t) \quad (5)$$

where $w_0 = 0.2$ and $w_1 = 0.8$. The AVP-weighted combination suppresses isolated noise points while preserving the high-contrast response of MIP for fine vessels. Layer boundaries are obtained by interpolating the pre-fitted curves to adaptively track retinal curvature and avoid inter-layer aliasing.

(3) Stripe removal: After normalizing the projection image, the column-wise median offset (referenced to the global median) is subtracted from each column to eliminate vertical bright-dark stripe artifacts caused by scan inconsistencies.

(4) CLAHE adaptive enhancement: Contrast-limited adaptive histogram equalization (CLAHE, clip limit = 0.01, tile grid = 10×10) is applied to the de-striped image to enhance local vascular contrast. The image is then horizontally flipped to align coordinate orientation with clinical convention.

(5) FAZ gradient processing: To address over-enhancement artifacts in the foveal avascular zone (FAZ) after CLAHE, an interactively delineated FAZ polygon is used as the seed region. The Euclidean distance from each pixel to the mask interior boundary is computed, and a cosine gradient weight map is constructed:

$$w(p) = c + (1 - c) \cdot cos^2(\pi \cdot d(p) / 2d\_max) \quad (6)$$

where c = 0.05 is the minimum center value, d(p) is the distance from pixel p to the FAZ mask boundary, and d_max is the maximum distance within the mask. A 12-pixel-wide feathering transition band is set outside the FAZ, and Gaussian smoothing (σ = 3) is applied to eliminate jagged edges, achieving a natural darkening transition in the FAZ region.

2.6 Two-stage Algorithm Architecture

The overall architecture of the proposed two-stage algorithm is shown in Figure 1. After MDMP removes systematic motion artifacts, the En-face enhancement pipeline operates on cleaner data, yielding higher contrast and sharper vascular images. The input data partitioning is summarized in Table 1.

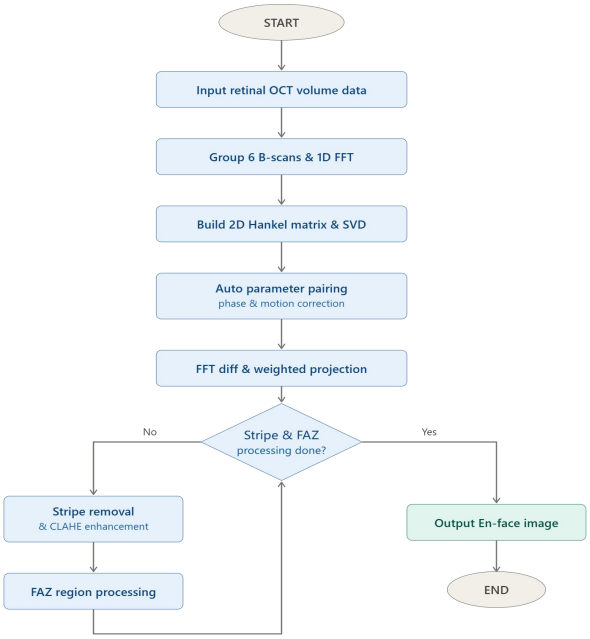

Figure 1 Overall Framework of the Proposed Two-stage MDMP and En-face Image Enhancement Algorithm

Table 1 Input Data Partitioning and Processing Pipeline

Stage	Data Type	Processing Method	Output Dimension	Function
Stage 1	A-scan sequence	2D matrix pencil construction	(L×K, N−L+1)	Parameter estimation
Stage 1	Enhanced matrix	Unitary transform / SVD	(2LK, 2(N−L+1))	Dimensionality reduction
Stage 1	Eigenvectors	Automatic pairing	(P, 3)	Motion compensation
Stage 2	Compensated volume	FFT difference + weighted projection	(256, 255)	En-face projection
Stage 2	Projected image	CLAHE + stripe removal + FAZ	(256, 255)	Image enhancement

3 EXPERIMENTS AND RESULTS

3.1 Experimental Setup

Experimental data were acquired from a commercial SD-OCT system (central wavelength 840 nm, axial resolution 5 μm, lateral resolution 15 μm). The dataset consists of retinal OCTA data with 2048×256×1530 voxels; each group contains six consecutive B-scans for blood flow signal extraction.

Algorithm parameters were set as follows: MDMP parameters L = 4, K = 4, P = 6; En-face enhancement parameters: MIP weight w_0 = 0.2, AVP weight w_1 = 0.8, Gaussian filter σ = 0.01, CLAHE clip limit = 0.01 with 10×10 tiles, FAZ feathering width = 12 pixels, minimum center value c = 0.05, and gradient smoothing σ = 3. Experiments were conducted on a workstation equipped with an Intel Core i7-12700 processor and 16 GB RAM; the algorithm was implemented in MATLAB R2022a.

3.2 Comparative Experiments

Six representative comparison methods were selected to validate the proposed approach: (1) no compensation; (2) phase difference; (3) SNR-weighted enhancement; (4) squared difference; (5) MDMP only; (6) the proposed method. The resulting En-face images are shown in Figure 2.

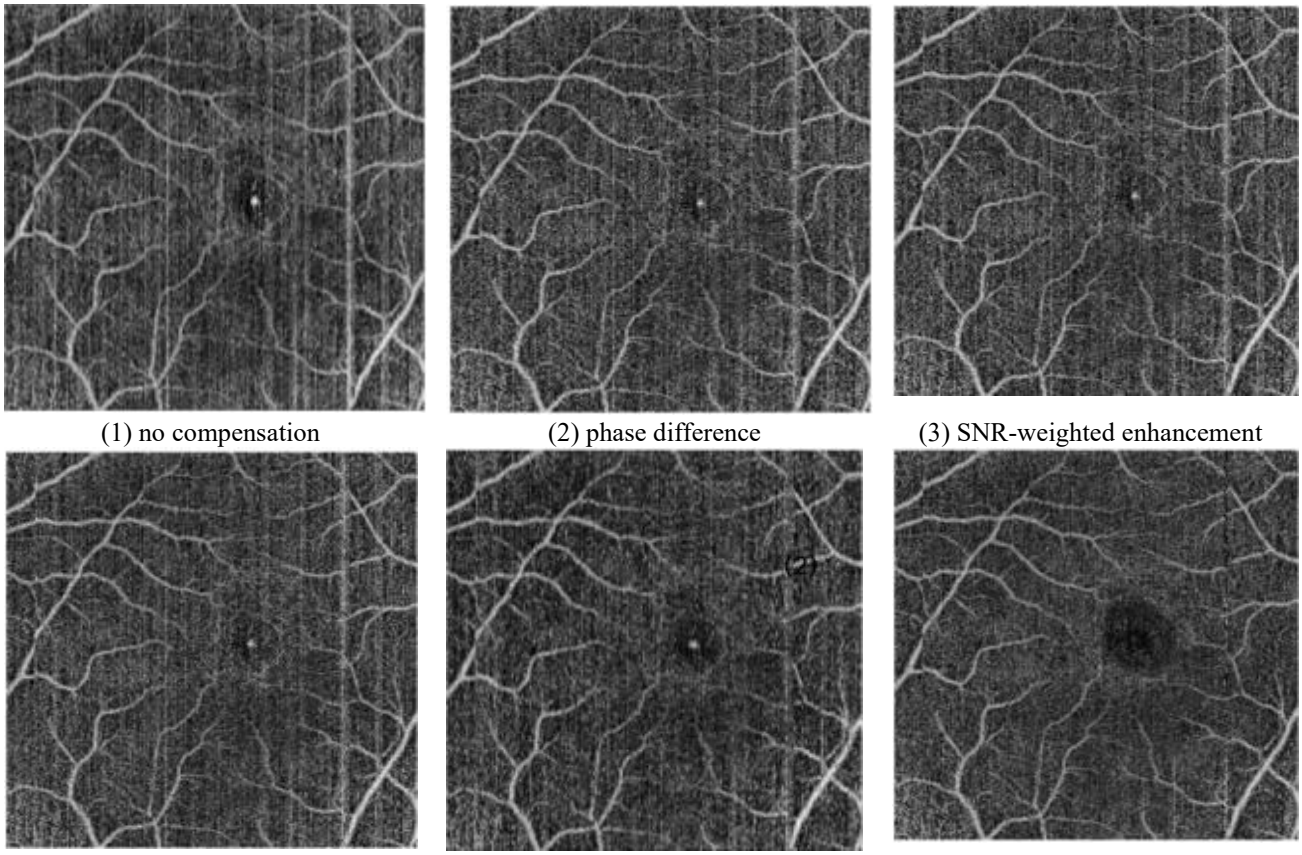

(1) no compensation (2) phase difference (3) SNR-weighted enhancement

(4) squared difference (5) MDMP only (6) proposed method

Figure 2 En-face Images Produced by the Compared Methods

The quantitative results are summarized in Table 2.

Table 2 Comprehensive Comparison of Motion Compensation Results

Method	SNR (dB)	CNR	SSIM	MAI
No compensation	10.33	1.865	0.65	0.106
Phase difference	10.75	1.927	0.76	0.094
SNR enhancement	11.83	2.204	0.81	0.078
Squared difference	12.09	2.361	0.86	0.098
MDMP only	14.41	3.291	0.92	0.074
Proposed method	17.06	3.36	0.94	0.07

As shown in Table 2, the proposed two-stage method achieves the best performance on all evaluation metrics. Compared with the no-compensation baseline, SNR improves by 65.1% (10.33 → 17.06 dB), CNR improves by 80.2% (1.865 → 3.36), SSIM increases from 0.65 to 0.94, and MAI decreases by 34.0% (0.106 → 0.07). Compared with the MDMP-only method, adding the En-face enhancement pipeline provides an additional 18.4% SNR improvement and raises SSIM from 0.92 to 0.94, confirming the significant contribution of the second-stage weighted layered projection and enhancement processing to En-face image quality.

3.3 Two-stage Incremental Analysis

Table 3 presents an incremental ablation analysis of the two processing stages.

Table 3 Incremental Effect Analysis of the Two-stage Processing

Configuration	SNR (dB)	SSIM	Description
Original image	10.33	0.65	No processing
Stage 1 only (MDMP)	14.41	0.92	Motion compensation
Stage 2 only (En-face enhancement)	10.72	0.74	En-face enhancement
Stage 1 + Stage 2	17.06	0.94	Full two-stage method

The ablation study shows that: (1) Stage 1 alone (MDMP) improves SNR from 10.33 dB to 14.41 dB (+39.5%), representing the primary performance gain; (2) Stage 2 alone applied directly to raw images yields an SNR of 10.72 dB and SSIM of 0.74, demonstrating that the enhancement pipeline itself is effective but limited without motion compensation support; (3) the full two-stage pipeline, compared with MDMP alone, provides an additional 18.4% SNR gain and raises SSIM from 0.92 to 0.94, confirming the necessity of the En-face enhancement stage on top of motion compensation.

4 CONCLUSIONS

This paper has presented a two-stage OCTA algorithm that combines the multi-dimensional matrix pencil method with En-face image enhancement. The first stage constructs a two-dimensional Hankel matrix pencil in the depth-time domain to jointly estimate motion parameters, reduces computational complexity by 75% via unitary transformation, and introduces an automatic parameter pairing mechanism to ensure correct parameter estimation. The second stage applies an En-face image enhancement pipeline to the MDMP-compensated volume data, sequentially performing FFT difference calculation, weighted layered projection (MIP×0.2 + AVP×0.8), CLAHE adaptive enhancement, column-wise median normalization for stripe removal, and FAZ cosine gradient darkening to generate high-quality En-face vascular images.

Experimental results on a retinal OCTA dataset show that, compared with conventional methods, the proposed approach achieves a 65.1% improvement in SNR, an 80.2% improvement in CNR, an SSIM of 0.94, and a 34.0% reduction in MAI. The two stages form a functionally complementary pipeline: MDMP eliminates systematic motion artifacts while the En-face enhancement pipeline maximizes vascular imaging quality on clean data, yielding superior accuracy and robustness.

Future work will explore the following directions: (1) adaptive parameter selection strategies for fully automatic processing; (2) GPU-based parallel acceleration to support real-time processing; (3) extension of the algorithm to three-dimensional motion compensation; and (4) integration of deep learning approaches for end-to-end motion compensation networks.

COMPETING INTERESTS

The authors have no relevant financial or non-financial interests to disclose.

REFERENCES

[1] Spaide RF, Fujimoto JG, Waheed NK, et al. Optical coherence tomography angiography. Progress in Retinal and Eye Research, 2018, 64: 1-55. DOI: 10.1016/j.preteyeres.2017.11.003.

[2] Kashani AH, Chen CL, Gahm JK, et al. Optical coherence tomography angiography: A comprehensive review of current methods and clinical applications. Progress in Retinal and Eye Research, 2017, 60: 66-100. DOI: 10.1016/j.preteyeres.2017.07.002.

[3] Javed A, Khanna A, Palmer E, et al. Optical coherence tomography angiography: a review of the current literature. Therapeutic Advances in Ophthalmology, 2023, 15: 1-16. DOI: 10.1177/03000605231187933.

[4] Chen CL, Wang RK. Optical coherence tomography based angiography. Biomedical Optics Express, 2017, 8(2): 1056-1082. DOI: 10.1364/BOE.8.001056.

[5] Li Y, Chen S, Ji L, et al. Intensity-differential optical coherence tomography angiography. Journal of Biomedical Optics, 2019, 24(6): 066003. DOI: 10.1117/1.JBO.24.6.066003.

[6] Anvari P, Ashrafkhorasani M, Habibi A, et al. Artifacts in Optical Coherence Tomography Angiography. Journal of Ophthalmic and Vision Research, 2021, 16(2): 271-286. DOI: 10.18502/jovr.v16i2.9091.

[7] Hormel TT, Huang D, Jia Y. Artifacts and artifact removal in optical coherence tomographic angiography. Quantitative Imaging in Medicine and Surgery, 2021, 11(3): 1120-1133. DOI: 10.21037/qims-20-730.

[8] Camino A, Zhang M, Dongye C, et al. Automated registration and enhanced processing of clinical optical coherence tomography angiography. Quantitative Imaging in Medicine and Surgery, 2016, 6(4): 391-401. DOI: 10.21037/qims.2016.07.02.

[9] Zhang M, Hwang TS, Campbell JP, et al. Projection-resolved optical coherence tomographic angiography. Biomedical Optics Express, 2016, 7(3): 816-828. DOI: 10.1364/BOE.7.000816.

[10] Wei X, Hormel TT, Guo Y, et al. High-resolution wide-field OCT angiography with a self-navigation method to correct microsaccades and blinks. Biomedical Optics Express, 2020, 11(6): 3234-3245. DOI: 10.1364/BOE.390801.
[11] Hossbach J, Husvogt L, Kraus MF, et al. Efficient and high accuracy 3-D OCT angiography motion correction in pathology. Biomedical Optics Express, 2021, 12(1): 974-989. DOI: 10.1364/BOE.411117.
[12] Li A, Du C, Pan Y. Deep-learning-based motion correction in optical coherence tomography angiography. Journal of Biophotonics, 2021, 14(12): e202100097. DOI: 10.1002/jbio.202100097.
[13] Li W, Yin H, Qin Z, et al. A multi-dimensional matrix pencil-based channel prediction method for massive MIMO with mobility. IEEE Transactions on Communications, 2023, 71(5): 2748-2762. DOI: 10.1109/TCOMM.2022.3214853.
[14] Sun Y, Ma Y, Zhao G, et al. An ASC-based unitary matrix pencil method for parameter estimation of group target. Radio Science, 2023, 58(7): e2022RS007649. DOI: 10.1029/2022RS007649.